Supplemental material

Isensee et al., https://doi.org/10.1083/jcb.201708053

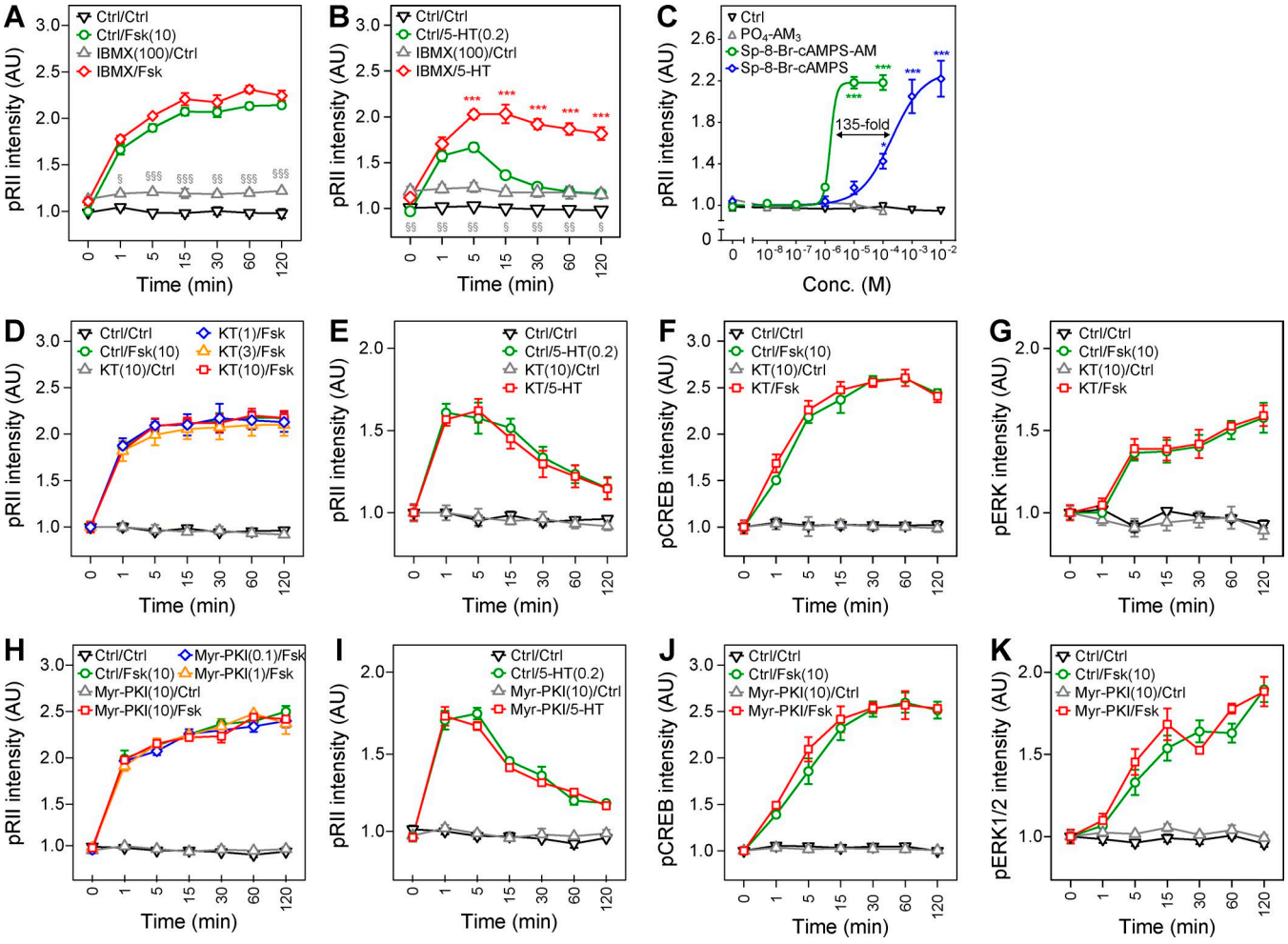

Figure S1. **KT5720 and Myr-PKI cannot inhibit the induction of pRII intensity and PKA downstream signaling in sensory neurons. (A)** Fsk-induced pRII response after pretreatment with 100 µM IBMX (30 min). IBMX alone increased the basal level of pRII intensity, but not the response to Fsk. **(B)** Effect of 100 µM IBMX (10-min pretreatment) on the transient induction of pRII intensity by 5-HT. IBMX amplified and prolonged the 5-HT response. **(C)** Dose-dependent induction of pRII intensity after stimulation (5 min) with the PKA agonists Sp-8-Br-cAMPS versus the cell-permeable Sp-8-Br-cAMPS-AM. The EC_{50} value of the unconjugated parent compound Sp-8-Br-cAMPS was 135-fold higher than that of the AM ester. The membrane-permeant, metabolically activatable phosphate PO_4-AM_3 used as a negative control did not induce a pRII response. **(D and E)** Time course of pRII intensity induced by Fsk (E) or 5-HT (F) after pretreatment with 1–10 µM KT5720 (30 min). **(F and G)** Pretreatment with KT5720 did not inhibit PKA downstream signaling such as the phosphorylation of CREB (C) and ERK1/2 (D). **(H and I)** Myristoylated protein kinase inhibitor peptide (Myr-PKI) did not inhibit the induction of pRII intensity by Fsk (E) or 5-HT (F). **(J and K)** Myr-PKI did not block PKA-downstream signaling at the level of CREB (G) or ERK1/2 phosphorylation (H). Values are means ± SEM; *n* = 3–4; >1,000 neurons/condition; two-way ANOVA with Bonferroni's test. ***, P < 0.001 indicate significance levels between stimulated conditions; §, P < 0.05; §§, P < 0.01; §§§, P < 0.001 indicate significance levels between basal conditions. Kinetic experiments are plotted in nonlinear scale.

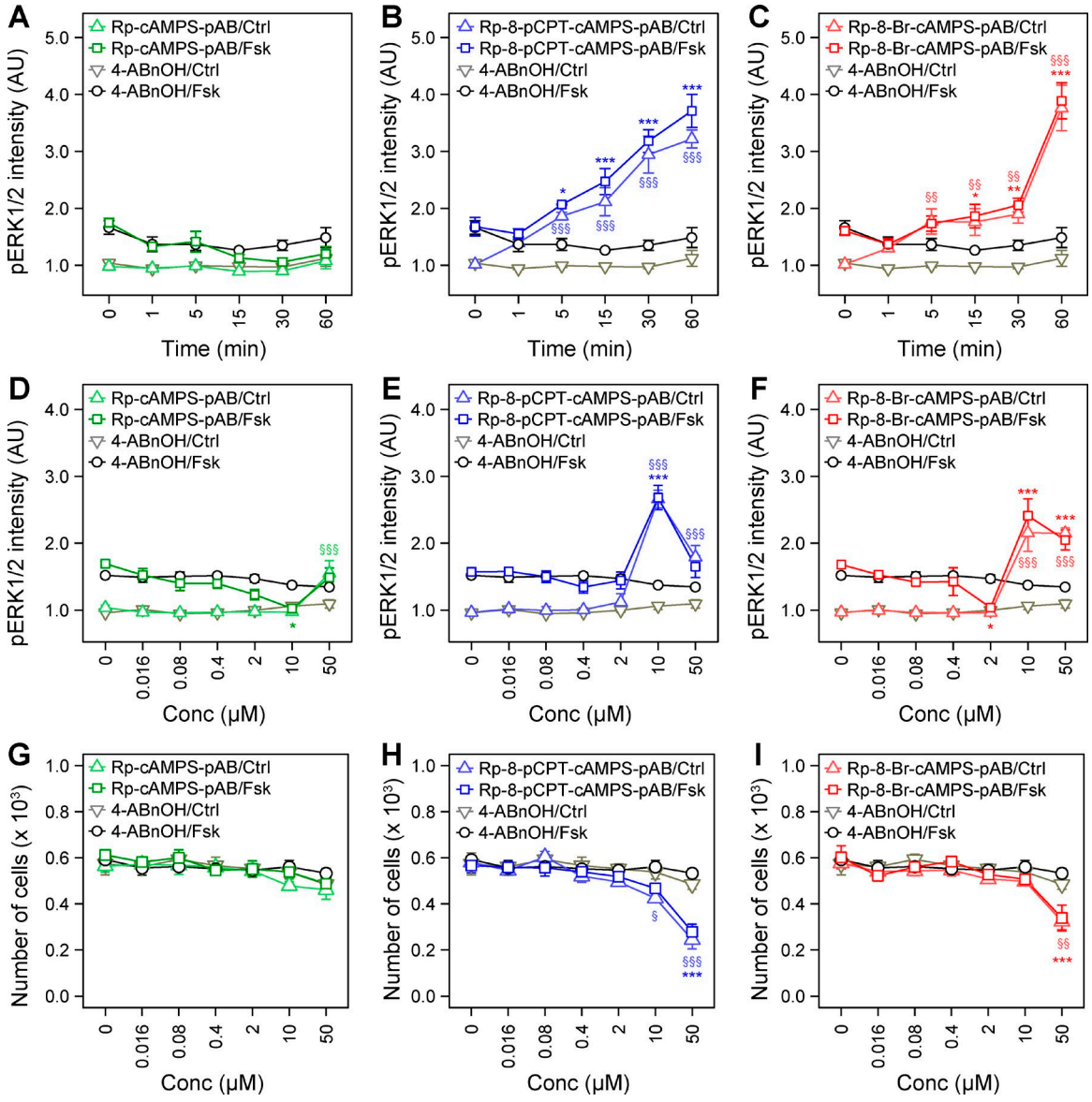

Figure S2. **At high concentrations, stimulation with Rp-isomers induce the phosphorylation of ERK1/2 and cell loss depending on their modification at position 8 of the adenine nucleobase. (A–C)** HCS microscopy analyses of pERK1/2 immunoreactivity after pretreatment of sensory neurons for up to 60 min with 10 µM Rp-cAMPS-pAB (A), Rp-8-pCPT-cAMPS-pAB (B), or Rp-8-Br-cAMPS-pAB (C) with or without subsequent 10 µM Fsk stimulation (5 min). 10 µM 4-ABnOH served as negative control. Rp-cAMPS-pAB had an inhibitory effect on the Fsk-induced cross talk to ERK1/2 (A). In contrast, treatment with Rp-8-Br-cAMPS-pAB or Rp-8-pCPT-cAMPS-pAB led to substantial phosphorylation of ERK1/2 (B and C). **(D–F)** Dose–response experiments after 30-min pretreatment with Rp-isomers followed by stimulation with 10 µM Fsk (5 min). Induction of ERK1/2 required significantly higher concentrations of Rp-cAMPS-pAB compared with both other compounds. **(G–I)** Pretreatment of sensory neurons with higher doses of pAB-conjugated Rp-isomers having modifications at position 8 of the adenine nucleobase decreased the number of analyzable neurons indicating cytotoxicity. Values represent means ± SEM; $n = 3–4$; >1,000 neurons/condition; one-way ANOVA with Bonferroni's posttest. *, $P < 0.05$; **, $P < 0.01$; ***, $P < 0.001$ indicate significance levels between Fsk-stimulated conditions; §, $P < 0.05$; §§, $P < 0.01$; §§§, $P < 0.001$ indicate significance levels between basal conditions.

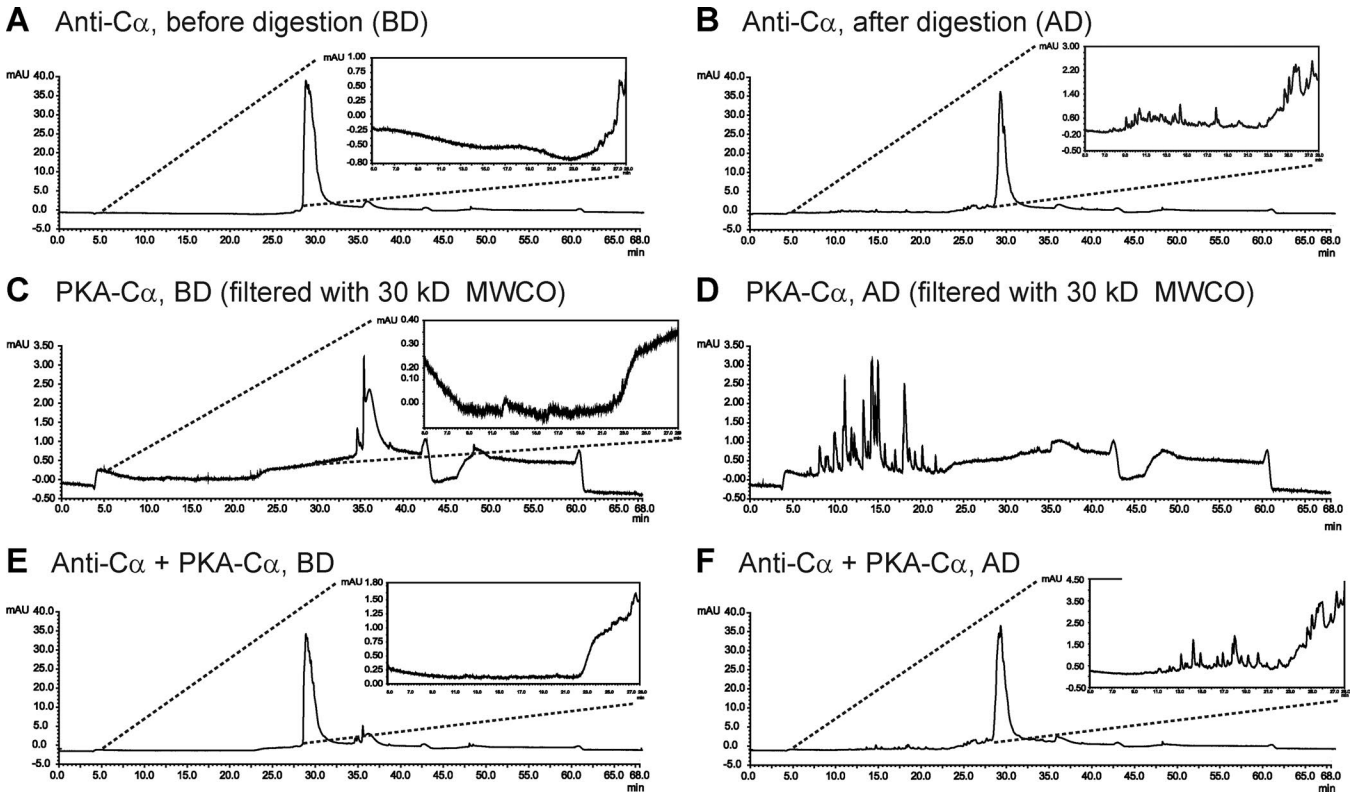

Figure S3. **Monolithic HPLC pre- and postdigestion controls for the anti–Cα antibody, PKA-Cα subunits, and coincubations thereof.** The magnified UV trace areas show where peptides elute, whereas proteins elute later at ∼30–35 min. **(A and B)** As expected, the anti–Cα antibody is largely resistant to subtilisin treatment. **(C and D)** In contrast, subtilisin treatment effectively fragments PKA-Cα subunits to peptides. **(E and F)** Coincubations of anti–Cα antibodies and PKA-Cα subunits before (E) and after (F) digestion with subtilisin. Samples from F were used for nano–LC-MS/MS. MWCO, molecular weight cutoff.

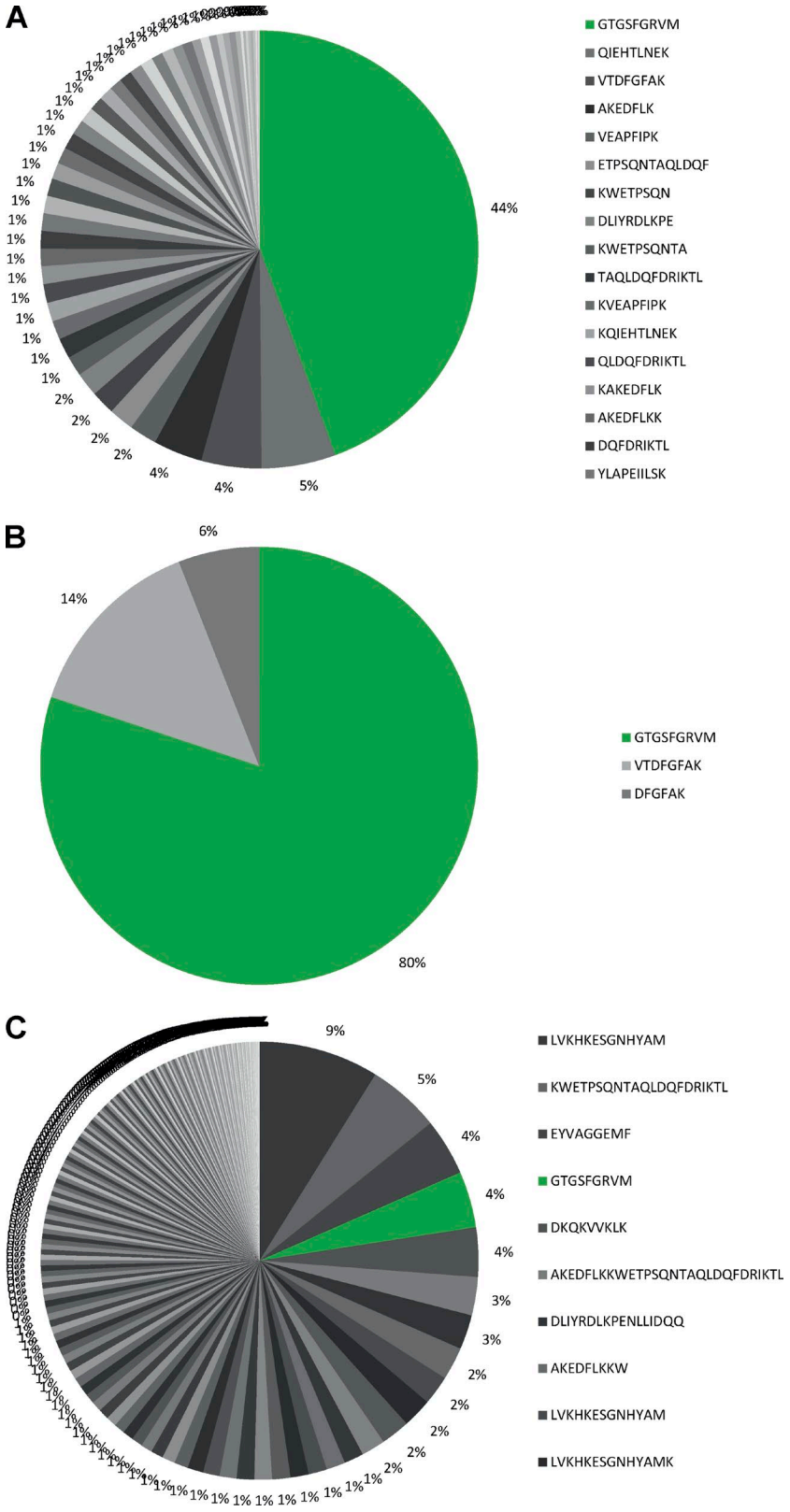

Figure S4. **Distribution of PSMs identified by LC-MS analysis as a measure of peptide abundance shows that the sequence GTGSFGRVM binds to the anti–Cα antibody. (A)** Proteolytic digestion of anti–Cα bound PKA-Cα subunits and removal of nonbound sequence parts before elution from the antibody leads to clear overrepresentation of GTGSFGRVM as compared with all other identified sequences. The minor presence of other sequences may be attributed to insufficient removal during the washing procedure. **(B)** GTGSFGRVM is confirmed in by alternative approach, where PKA-Cα subunits were first digested and then incubated with anti–Cα antibodies. Nonbound peptides were removed before LC-MS analysis of the eluate. **(C)** PSM distribution of a PKA-Cα subtilisin digest without antibody treatment.

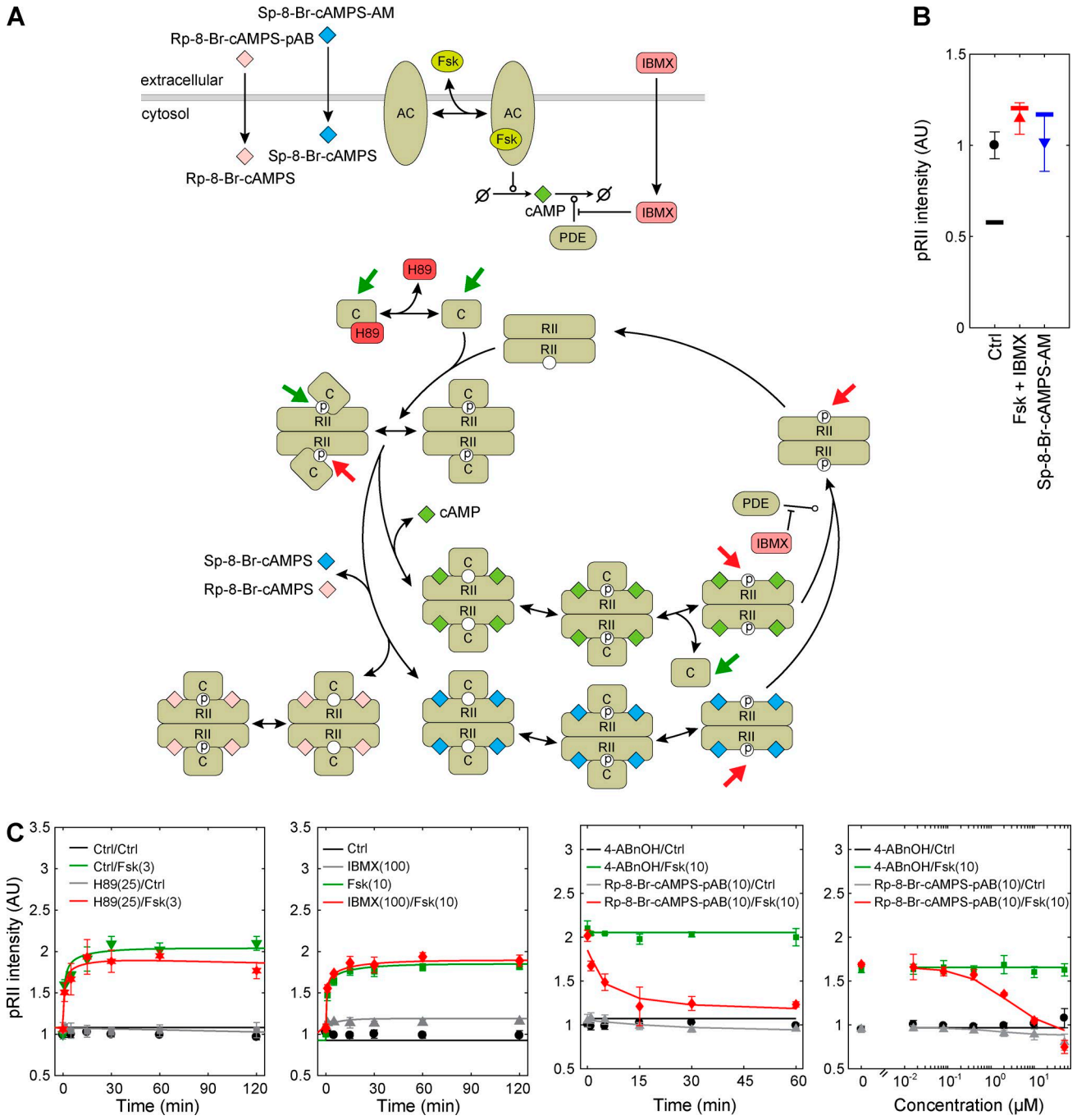

Figure S5. **An alternative model structure, which assumes that cAMP induces RII phosphorylation, cannot describe the Western blot data. (A)** Illustration of an alternative model structure assuming that cAMP induces RII phosphorylation. Colored arrows indicate the epitopes recognized by the rb-pRII (red) and mo-Cα (green) antibodies, respectively. **(B and C)** Comparison of experimental data obtained using Western blotting of cell lysates (B) or immunostaining of intact neurons (C) with simulation results using the alternative model. The alternative model describes the immunostaining data, but not the Western blot data. Immunoblot results in B are means ± SD; *n* = 6. HCS results in C represent means ± SEM; *n* = 3–4; >1,000 neurons/condition.

Provided online as a ZIP file is the supplemental modeling archive including the used experimental data, Data2Dynamics implementation, visualization of the fitting results, and best parameters found for each model. The archive is also available at https://doi.org/10.6084/m9.figshare.5991136.v2.